Analysis of the Effects of Boron Transient Enhanced Diffusion on Threshold Voltage Mismatch in Steep Retrograde Doping NMOSFETs with Inserted Oxygen Layers

Shuntaro Fujii[1], Hideki Takeuchi[2], Soichi Morita[1], Tatsushi Yagi[1], Shohei Hamada[1], Toshiro Sakamoto[1], Shinji Kawaguchi[1], Naoki Ishigami[1], Atsushi Okamoto[1], Shuji Ikeda[3], Hiu-Yung Wong[4], Robert J. Mears[2], and Tsutomu Miyazaki[1]
[1]Process Technology & Development, Asahi Kasei Microsystems, 5-4960 Nakagawara, Nobeoka, Japan
[2]Atomera, 750 Uniersity Avenue, Suite 280, Los Gatos, USA
[3]tei solutions, 16-1 Onogawa, Tsukuba, Japan
[4]San Jose State University, One Washington Square, San Jose, USA
Phone : +81-982-22-5252, Email : fujii.sv@om.asahi-kasei.co.jp

***Abstract*— Steep retrograde doping devices were fabricated using undoped epitaxial Si channels with inserted oxygen layers. The effects of boron transient enhanced diffusion (TED) on threshold voltage (V_{th}) mismatch were investigated. Suppression of boron TED was effective for reducing V_{th} mismatch of steep retrograde doping devices as well as flat doping profile devices.**

Keywords*— *V_{th} mismatch, Retrograde doping, Undoped epitaxial channel, Boron, Transient enhanced diffusion

I. Introduction

Threshold voltage (V_{th}) variation has become a serious issue in planar devices [1]. Various V_{th} variation sources have been reported such as random dopant fluctuation (RDF) [2], the gate oxide thickness [3], line edge roughness of the gate electrodes [4], variation of gate crystallinity [5], depletion of gate poly-Si [6], halo implantation [7], and interface state density and fixed oxide charges [8]. Among them, RDF has the largest impact on V_{th} variation [1]. Furthermore, it has been reported that V_{th} variation in NMOSFETs is larger than that in PMOSFETs due to transient enhanced diffusion (TED) of channel boron atoms. The discussion is based on V_{th} dependences on gate width and back bias (V_b) [9].

It has been reported that steeper retrograde doping profiles can reduce RDF [10]. Undoped epitaxial Si growth on active regions incorporating a carbon-doped diffusion blocking layer can result in steeper doing profiles [11]. Thicker undoped Si thickness (T_{epi}) is also effective [12]. However, the effect of boron TED on V_{th} variation in undoped epitaxial Si channel devices has not been reported.

In this work, firstly, the effect of boron TED on V_{th} mismatch of paired devices ($\sigma\Delta V_{th}$) was studied further using NMOSFETs without boron TED. In the next, undoped epitaxial Si channel NMOSFETs were fabricated. The effects of boron TED on $\sigma\Delta V_{th}$ were investigated by changing extension and deep source/drain (S/D) conditions.

II. Experiments

Fig. 1 shows the sample preparation flow. NMOSFETs were fabricated on Si (100) wafers. Channel direction was <110>. To eliminate boron TED induced by extension and deep S/D implantation, channel implantation was carried out after S/D activation for post-S/D V_{th}-controlled devices [13]. NMOSFETs with or without undoped epitaxial Si growth were fabricated. Fig. 2 shows the cross-sectional schematic images of the devices. It has been shown that inserted oxygen layers can inhibit diffusion of dopants to Si surface because of a strong interaction of the inserted oxygen layers with interstitial silicon (I-Si) atoms [14]. The other effect of inserted oxygen layers than I-Si trapping is electron sub-band repopulation for increase of effective electron mobility (μ_{eff}) [15]. Undoped epitaxial Si channels with inserted oxygen layers were therefore grown on active regions after channel activation. The gate oxide film was SiO_2 with an electrical thickness in strong inversion (T_{inv}) of 3.8 nm. It is known that the degree of boron TED depends on activation annealing conditions [16]. After extension and deep S/D implantation steps, rapid thermal annealing (RTA) was carried out at 992°C for 10 s with the ramping rate of 75°C/s for this study. Halo implantation was skipped. The devices were evaluated in linear region with drain voltage of 50 mV or 0.1 V.

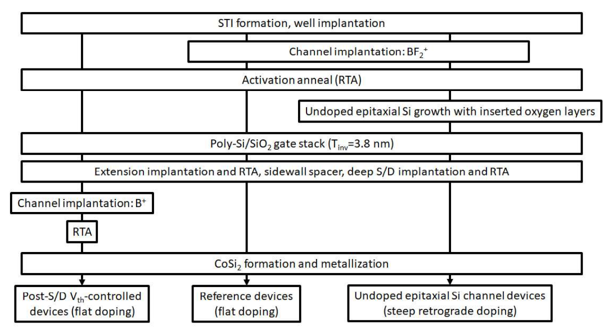

Fig. 1. Sample preparation flow.

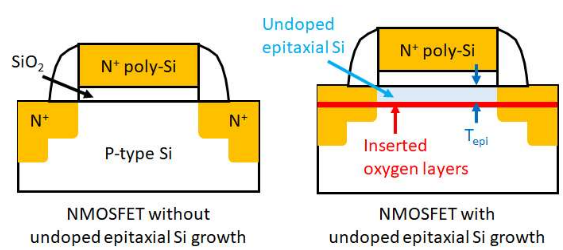

Fig. 2. Cross-sectional schematic images of the devices.

III. Results and Discussion

Fig. 3 shows V_{th} dependences on the designed gate length (L_g) of the reference devices and post-S/D V_{th}-controlled devices. The designed gate width (W_g) of the reference devices was from 0.2 µm to 10 µm. Post-S/D V_{th}-controlled devices did not show reverse short channel effect (RSCE) since boron TED was eliminated. In the reference devices, both RSCE and reverse narrow channel effect were observed since TED makes boron concentration near the extension regions higher and that near the active corners lower. To focus on the impact of the higher boron concentration regions near the extension regions on $\sigma\Delta V_{th}$, the devices with W_g of 0.5 μm and wider were evaluated. Fig. 4 shows $\sigma\Delta V_{th}$ of the reference devices and post-S/D V_{th}-controlled devices. It was directly demonstrated that boron pileup near the extension regions induced by TED degraded $\sigma\Delta V_{th}$.

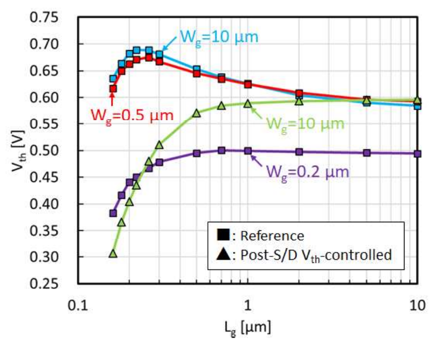

Fig. 3. V_{th} dependences on L_g of the reference devices and post-S/D V_{th}-controlled devices.

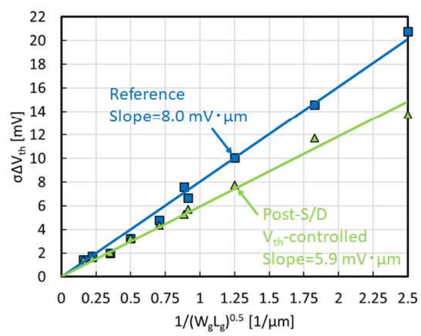

Fig. 4. $\sigma\Delta V_{th}$ dependences on channel size of the reference devices and post-S/D V_{th}-controlled devices. 153 paired devices were measured.

Fig. 5 shows μ_{eff} dependences on effective electrical field (E_{eff}) of the epitaxial Si channel devices with various T_{epi} at room temperature. μ_{eff} was characterized using split CV method. T_{epi} was varied from 5 nm to 15 nm. Channel dose was constant for all samples. At low E_{eff}, μ_{eff} became higher with thicker T_{epi} since impurity scattering was suppressed [17]. On the other hand, at high E_{eff}, μ_{eff} became higher with thinner T_{epi} since the effect of electron population to Δ-2 valleys induced by inserted oxygen layers becomes larger in thinner T_{epi} [15]. This result suggested successful integration of undoped epitaxial Si channels with inserted oxygen layers.

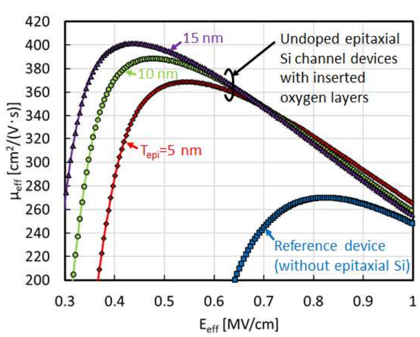

Fig. 5. μ_{eff} dependences on E_{eff} with various T_{epi}.

Fig. 6 shows V_{th} dependences on channel BF_2^+ dose. Both L_g and W_g were 10 μm. To match V_{th}, the epitaxial Si channel devices required higher channel dose than the reference devices. Fig. 7 shows V_{th} dependences on L_g with various T_{epi}. Channel dose was increased for the epitaxial Si channel devices to match V_{th} at long L_g as shown in Fig. 6. Arsenic ions were implanted into extension and deep S/D regions. The epitaxial Si channel devices showed stronger RSCE than the reference devices as T_{epi} became thicker.

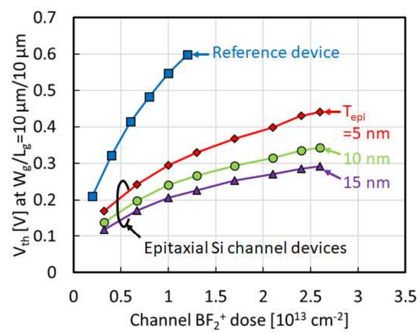

Fig. 6. V_{th} dependences on channel BF_2^+ dose with various T_{epi} at W_g/L_g=10 μm/10 μm.

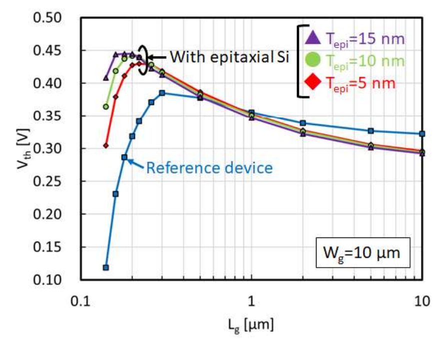

Fig. 7. V_{th} dependences on L_g with various T_{epi}. Channel dose was tuned to match long channel V_{th}.

Using blanket wafers, boron depth profiles were investigated. Fig. 8 shows SIMS results of boron depth profiles in the channel, extension, and deep S/D regions of the epitaxial Si channel devices. T_{epi} was 25 nm. Arsenic ions were implanted into the extension and deep S/D regions. The channel profile of the reference device is also shown. Channel BF_2^+ dose was constant for all wafers. Using inserted oxygen layers, steep retrograde doping profile was formed in the channel region. In the extension and deep S/D regions, however, boron diffusion to Si surface was observed. It was found that the origin of RSCE in the epitaxial Si channel devices was induced by TED of boron atoms. In addition, it was suggested that higher boron concentration under the epitaxial Si films than the reference devices enhanced RSCE.

To suppress RSCE, extension and deep S/D implantation conditions were modified to reduce the number of I-Si atoms. Fig. 9 shows process simulation results for the depth profiles of I-Si atoms in extension and deep S/D regions. The number of I-Si atoms can be reduced by reducing dose and changing ions from As^+ to P^+. Fig. 10 shows V_{th} dependences on L_g with various extension and deep S/D implantation conditions for T_{epi} of 5 nm and 10 nm. Both extension and deep S/D implantation conditions had impacts on V_{th}-L_g characteristics. RSCE was successfully suppressed by reducing the number of I-Si atoms for both T_{epi} cases.

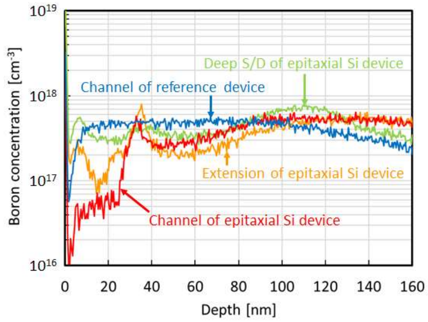

Fig. 8. Boron profiles in the channel, extension, and deep S/D regions of the epitaxial Si channel devices with T_{epi}=25 nm.

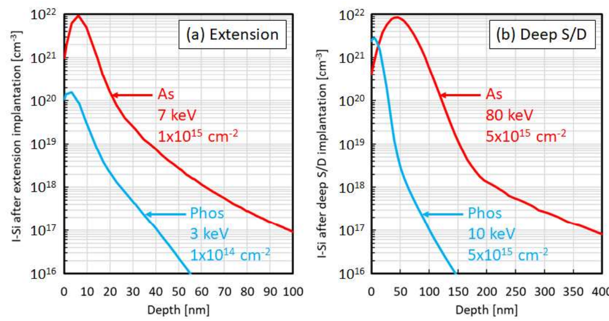

Fig. 9. Simulated depth profiles of I-Si atoms in (a) extension and (b) deep S/D regions.

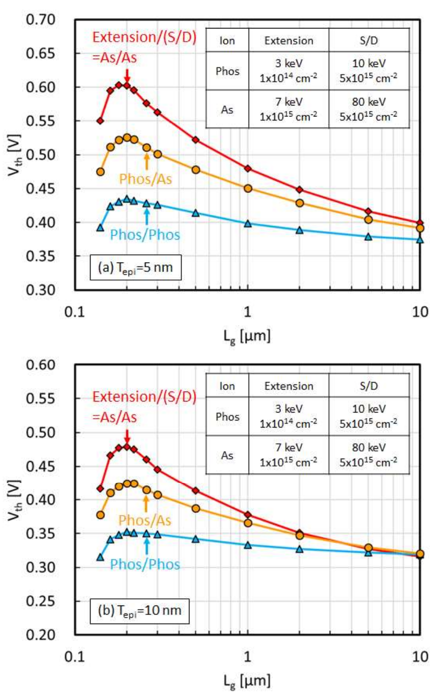

Fig. 10. V_{th} dependences on L_g with various extension and deep S/D conditions of the epitaxial Si channel devices. (a) T_{epi}=5 nm and (b) T_{epi}=10 nm. Channel dose was constant for each T_{epi}. W_g=10 μm

It has been reported that steepness of channel doping profiles can be evaluated using V_{th} dependences on V_b, body factor (γ) [11], [18]. Fig. 11 shows γ dependences on V_{th} for T_{epi}=5 nm and 10 nm. For both T_{epi} cases, the epitaxial Si channel devices showed larger γ than the reference devices at L_g=10 μm. This result suggests that channel doping profiles at the channel center of the epitaxial Si channel devices were steeper than those of the reference devices. At L_g=10 μm, γ of the epitaxial Si channel devices did not depend on extension and deep S/D implantation conditions. Whereas, at L_g=0.3 μm, γ of the epitaxial Si channel devices became smaller as RSCE became stronger. This result suggests that stronger RSCE conditions degraded steepness of channel doping profiles near the extension regions of the epitaxial Si channel devices.

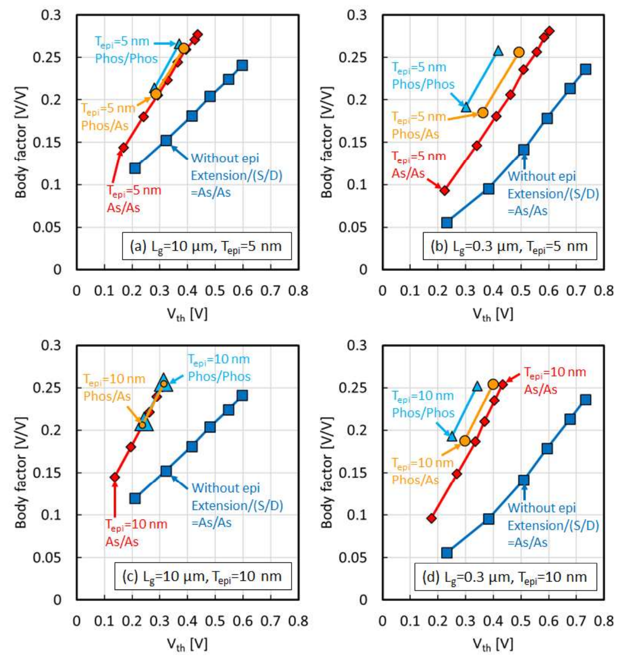

Fig. 11. Body factor dependences on V_{th} at (a) L_g=10 μm for T_{epi}=5 nm, (b) L_g=0.3 μm for T_{epi}=5 nm, (c) L_g=10 μm for T_{epi}=10 nm, and (d) L_g=0.3 μm for T_{epi}=10 nm. W_g=10 μm.

Fig. 12 shows typical results of $\sigma\Delta V_{th}$ of the epitaxial Si channel devices for T_{epi}=5 nm and 10 nm. Only extension and deep S/D conditions were changed. V_{th} mismatch was reduced by the epitaxial Si channels and by suppression of boron TED. Fig. 13 shows V_{th} mismatch slope dependences on V_{th}. It was found that suppression of TED to retain the steepness of channel doping profiles even near the extension regions was effective to reduce $\sigma\Delta V_{th}$ in the epitaxial Si channel devices. For increased T_{epi} up to 10 nm, V_{th} mismatch slope reduction by more than 50% was achieved at V_{th}~0.32 V.

In this study, boron TED was suppressed by reducing the number of I-Si atoms in extension and deep S/D implantation steps. But, this approach has a negative impact on device performance. Fig. 14 shows series resistance (R_{sd}) with different extension and deep S/D conditions. Smaller RSCE conditions degraded R_{sd}. As devices are scaled, higher R_{sd} degrades drain current severely. Therefore, other approaches to maintain low R_{sd} with suppressing RSCE are needed. It has been reported that higher ramping rate annealing [16] and carbon co-implantation [19] can suppress TED. In addition to undoped epitaxial Si growth with inserted oxygen layers, such technologies should be applied for reducing V_{th} variation.

IV. Conclusion

The effects of boron TED on V_{th} mismatch in undoped epitaxial Si channel NMOSFETs with inserted oxygen layers have been investigated. From RSCE, body factor, and SIMS results, it can be concluded that V_{th} mismatch in undoped epitaxial Si channel devices can be successfully reduced by suppressing boron TED to maintain steepness of channel doping profiles near the extension regions in addition to those at the channel center. V_{th} mismatch reduction of more than 50% at matched V_{th} for the epitaxial Si channel devices compared to the reference devices has been achieved. The results are useful for design of low V_{th} variation devices.

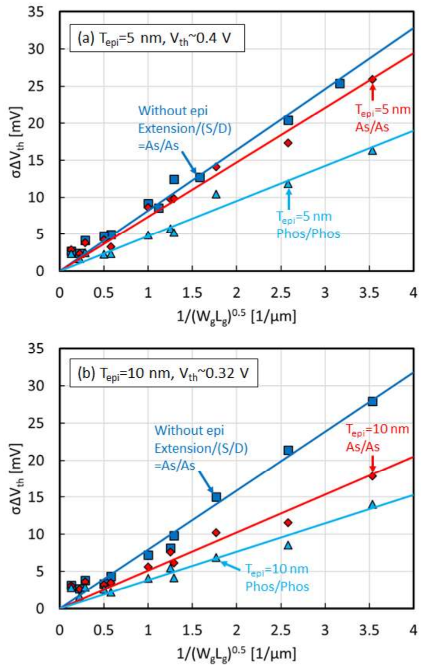

Fig. 12. Typical results of $\sigma\Delta V_{th}$ dependences on channel size of the epitaxial Si channel devices. (a) T_{epi}= 5 nm and (b) T_{epi}=10 nm. 45 paired devices were measured for each channel size.

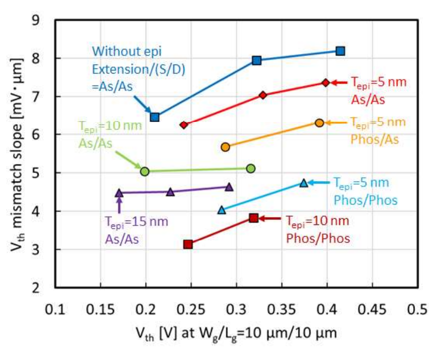

Fig. 13. $\sigma\Delta V_{th}$ slope dependences on V_{th} at W_g/L_g=10 μm/10 μm for the reference devices and the epitaxial Si channel devices.

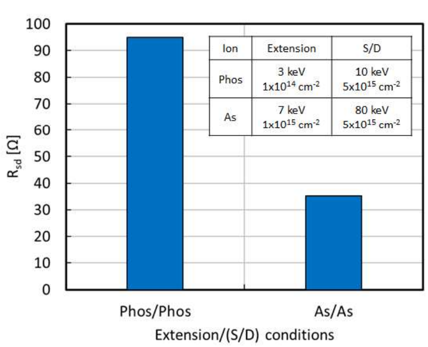

Fig. 14. R_{sd} with different extension and deep S/D conditions extracted from R_{on}-L_{mask} for W_g=10 μm.

REFERENCES

[1] T. Tsunomura, A. Nishida, and T. Hiramoto, "Analysis of NMOS and PMOS Difference in V_T variation With Large-Scale DMA-TEG," IEEE Trans. Electron Devices, vol. 56, pp. 2073-2080, 2009.

[2] K. Takeuchi, T. Fukai, T. Tsunomura, A. T. Putra, A. Nishida, S. Kamohara, and T. Hiramoto, "Understanding Random Threshold Voltage Fluctuation by Comparing Multiple Fabs and Technologies," in Proc. 2007 IEEE IEDM, pp. 467-470.

[3] A. Asenov, A. R. Brown, J. H. Davies, S. Kaya, and G. Slavcheva, "Simulation of Intrinsic Parameter Fluctuations in Decananometer and Nanometer-Scale MOSFETs," IEEE Trans. Electron Devices, vol. 50, pp. 1837-1852, 2003.

[4] A. Asenov, S. Kaya, and A. R. Brown, "Intrinsic Parameter Fluctuations in Decananometer MOSFETs Introduced by Gate Line Edge Roughness," IEEE Trans. Electron Devices, vol. 50, pp. 1254-1260, 2003.

[5] M. Saitoh, K. Ota, C. Tanaka, Y. Nakabayashi, K. Uchida, and T. Numata, "Performance, Variability and Reliability of Silicon Tri-Gate Nanowire MOSFETs," in Proc. 2012 IEEE IRPS, pp. 6A.3.1-6A.3.6.

[6] H. P. Tuinhout, A. H. Montree, J. Schmitz, and P. A. Stolk, "Effects of Gate Depletion and Boron Penetration on Matching of Deep Submicron CMOS Transistors," in Proc. 1997 IEEE IEDM, pp. 631-634.

[7] K. Takeuchi, A. Nishida, S. Kamohara, T. Hiramoto, and T. Mogami, "Proposal of a Model for Increased NFET Random Fluctuations," in Proc. 2011 VLSI Technology, pp. 192-193.

[8] T. Matsukawa, Y. Liu, W. Mizubayashi, J. Tsukada, H. Yamauchi, K. Endo, Y. Ishikawa, S. O'uchi, H. Ota, S. Migita, Y. Morita, and M. Masahara, "Suppressing V_t and G_m Variability of FinFETs Using Amorphous Metal Gates for 14 nm and Beyond," in Proc. 2012 IEEE IEDM, pp. 175-178.

[9] T. Tsunomura, A. Nishida, and T. Hiramoto, "Effect of Channel Dopant Profile on Difference in Threshold Voltage Variability Between NFETs and PFETs," IEEE Trans. Electron Devices, vol. 58, pp. 364-369, 2011.

[10] K. Takeuchi, T. Tatsumi, and A. Furukawa, "Channel Engineering for the Reduction of Random-Dopant-Placement-Induced Threshold Voltage Fluctuation," in Proc. 1997 IEEE IEDM, pp. 841-844.

[11] A. Hokazono, H. Itokawa, N. Kusunoki, I. Mizushima, S. Inaba, S. Kawanaka, and Y. Toyoshima, "25-nm Gate Length nMOSFET With Steep Channel Profiles Utilizing Carbon-Doped Silicon Layers (A P-Type Dopant Confinement Layer)," IEEE Trans. Electron Devices, vol. 58, pp. 1302-1310, 2011.

[12] A. Ghetti, S. M. Amoroso, A. Mauri, and C. M. Compagnoni, "Impact of Nonuniform Doping on Random Telegraph Noise in Flash Memory Devices," IEEE Trans. Electron Devices, vol. 59, pp. 309-315, 2012.

[13] S. Fujii, T. Yagi, S. Hamada, I. Maru, Y. Okuaki, T. Chiaki, A. Okamoto, T. Sakamoto, and T. Miyazaki, "Analyzing the Effects of Boron Transient Enhanced Diffusion on Low Frequency Noise in NMOSFETs," in Proc. 2017 IEEE IRPS, pp. XT-3.1-XT-3.5.

[14] R. J. Mears, H. Takeuchi, R. J. Stephenson, M. Hytha, R. Burton, N. W. Cody, D. Weeks, D. Choutov, N. Agrawal, and S. Datta, "Punch-Through Stop Doping Profile Control via Interstitial Trapping by Oxygen-Insertion Silicon Channel," in Proc. 2017 IEEE EDTM, pp. 65-66.

[15] N. Xu, H. Takeuchi, M. Hytha, N. W. Cody, R. J. Stephenson, B. Kwak, S. Y. Cha, R. J. Mears, and T. J. K. Liu, "Electron mobility enhancement in (100) oxygen-inserted silicon channel," Applied Physics Letters, vol. 107, pp. 123502-1-123502-5, 2015.

[16] A. Ono, R. Ueno, and I. Sakai, "TED Control Technology for Suppression of Reverse Narrow Channel Effect in 0.1 μm MOS Devices," in Proc. 1997 IEEE IEDM, pp. 227-230.

[17] S. Takagi, A. Toriumi, M. Iwase, and H. Tango, "On the Universality of Inversion Layer Mobility in Si MOSFET's: Part I-Effects of Substrate Impurity Concentration," IEEE Trans. Electron Devices, vol. 41, pp. 2357-2362, 1994.

[18] H. Koura, M. Takamiya, and T. Hiramoto, "Optimum Conditions of Body Effect Factor and Substrate Bias in Variable Threshold Voltage MOSFETs," Japanese Journal of Applied Physics, vol. 39, pp. 2312-2317, 2000.

[19] T. Tsunomura, A. Nishida, F. Yano, A. T. Putra, K. Takeuchi, S. Inaba, S. Kamohara, K. Terada, T. Mama, T. Hiramoto, and T. Mogami, "Analysis of Extra V_T Variability Sources in NMOS Using Takeuchi Plot," in Proc. 2009 VLSI Technology, pp. 110-111.